



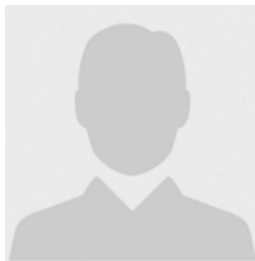
# Investigation of the Effects of Some Input Parameters on the Tensile Strength of Mild Steel Using RSM



Eyaefe Sunday <sup>a</sup>, Achebo J. I <sup>b</sup>, Obahiagbon K. O <sup>c</sup>, Etin-Osa C. E <sup>d</sup>

Manuscript submitted: 09 April 2026, Manuscript revised: 18 May 2026, Accepted for publication: 27 June 2026

## Corresponding Author <sup>a</sup>



## Abstract

Tensile strength has been a key measurement used by researchers, engineers, and quality control departments to evaluate the mechanical properties of a material, product, or component. This study aimed to investigate the effect of welding current, voltage, and travel speed on the tensile strength for Gas Metal Arc Welding (GMAW) of mild steel using Response Surface Methodology. A Central Composite Design comprising twenty experimental runs was employed to systematically investigate the effects of three input factors: welding current (180–210 A), voltage (22–25 V), and weld speed (2.0–3.5 mm/s). Quadratic polynomial models were developed using Response Surface Methodology in Design-Expert software. Multi-objective optimization was performed using both the desirability function approach within RSM. All optimized parameter combinations were experimentally validated through confirmation runs, with statistical diagnostics including coefficient of determination ( $R^2$ ), adjusted  $R^2$ , predicted  $R^2$ , lack-of-fit tests, and residual analysis used to assess model adequacy and predictive reliability. Results showed RSM predictive accuracy of tensile strength was 76.78%. The optimization approaches converged to a consistent optimal parameter window (Current  $\approx$ 194–195 A, Voltage = 25 V, Weld Speed  $\approx$ 2.7–3.5 mm/s).

## Keywords

current;  
gas;  
speed welding;  
tensile;  
voltage;

International Journal of Physical Sciences and Engineering © 2026.

This is an open access article under the CC BY-NC-ND license

(<https://creativecommons.org/licenses/by-nc-nd/4.0/>).

## Contents

Abstract.....	7
1 Introduction.....	8
2 Materials and Methods.....	8
3 Results and Discussions.....	10
4 Conclusion.....	14
Acknowledgments.....	14

<sup>a</sup> Department of Production Engineering, University of Benin, Benin City, Nigeria

<sup>b</sup> Department of Production Engineering, University of Benin, Benin City, Nigeria

<sup>c</sup> Department of Chemical Engineering, University of Benin, Benin City, Nigeria

<sup>d</sup> Department of Production Engineering, University of Benin, Benin City, Nigeria

---

References .....	15
Biography of Authors .....	16

---

---

## 1 Introduction

Welding remains one of the most indispensable fabrication processes in modern manufacturing, construction, automotive, shipbuilding, oil and gas, aerospace, and structural engineering industries. The ability to permanently join metallic components with high strength and reliability has enabled the creation of complex structures ranging from skyscrapers and bridges to pipelines, pressure vessels, and automobile chassis (Liu et al., 2013). Among the various materials available for these applications, mild steel (low-carbon steel containing approximately 0.05–0.25% carbon) is overwhelmingly the most widely utilized because of its exceptional combination of affordability, high ductility, excellent machinability, and, most importantly, superior weldability compared to higher-carbon or alloy steels. However, despite these favorable characteristics, welding operations inherently subject the base material to intense, localized heating and subsequent rapid cooling cycles (Achebo, 2012).

Mild steel, also known as low-carbon steel, is defined by its carbon content ranging from approximately 0.05% to 0.25% by weight, with the balance primarily iron and small amounts of manganese (0.3–0.6%), silicon (0.1–0.3%), and residual elements such as sulfur and phosphorus (each typically below 0.05%) (Achebo & Omoregie, 2013). This specific chemical composition places mild steel in a unique position among engineering materials: it offers an exceptional balance of mechanical properties, formability, weldability, and cost-effectiveness that few other materials can match. Unlike higher-carbon steels (0.3–0.6% C), which exhibit greater strength but reduced ductility and weldability, or alloy steels, which require special handling and post-weld heat treatment, mild steel can be reliably welded using virtually any arc welding process without preheating (except in very thick sections) or complex post-weld procedures (Achebo, 2011). Tensile strength and yield strength of welded mild steel joints are typically close to those of the base metal when welding parameters are properly selected (Achebo & Odinikuku, 2015). For a well-optimized weld with a narrow HAZ (1.5–2.5 mm), the joint efficiency (ratio of joint tensile strength to base metal tensile strength) is typically 95–100% (Sada et al., 2021).

## 2 Materials and Methods

Mild steel coupons were used in this study, as shown in Figure 1. Each specimen was precision-cut to dimensions of 150 mm × 50 mm × 6 mm using abrasive water-jet machining to minimize thermal pre-conditioning of the base metal, thereby preserving the as-received microstructure before welding.

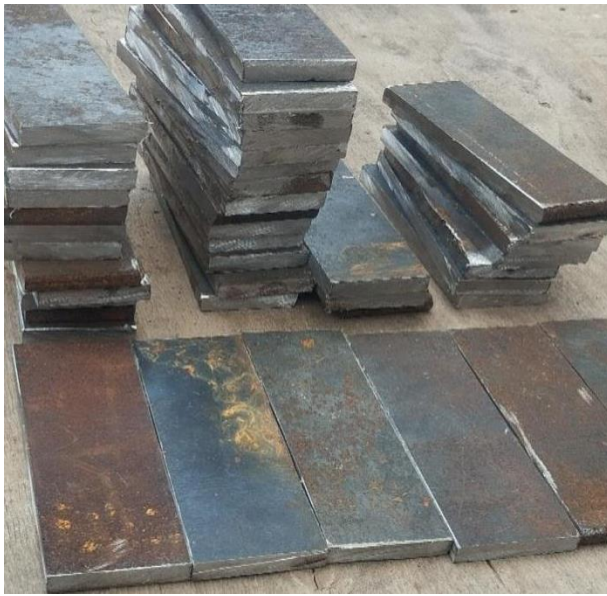


Figure 1: Mild Steel Coupons

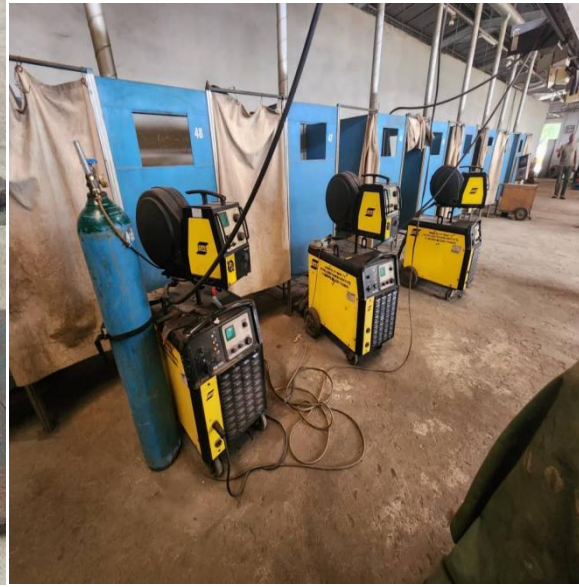


Figure 2: Welding Machine

Figure 2 depicts the semi-automated Gas Metal Arc Welding (GMAW) system utilized for all experimental welds, configured with a constant-voltage power source (Miller XMT® 350 CC/CV) capable of delivering stable current output within  $\pm 2\%$  tolerance across the 180–210 A operational range. The coded and uncoded levels of the three independent welding process variables, current (A), voltage (B), and weld speed (C), were selected for systematic investigation based on preliminary screening experiments and extant literature on GMAW of low-carbon steels (Palani & Murugan, 2006; Rao & Yadava, 2009). The factor ranges (Current: 180–210 A; Voltage: 22–25 V; Weld speed: 2.0–3.5 mm/s) were deliberately constrained to the stable globular-to-spray transition regime to avoid excessive spatter or incomplete fusion, while still encompassing industrially relevant parameter windows for structural fabrication. Coded values ( $-1$  to  $+1$ ) were derived via standard normalization  $x_{code} = 2(x - x_{min}) / (x_{max} - x_{min}) - 1$  to facilitate orthogonal polynomial regression in the Central Composite Design framework, with mean and standard deviation statistics confirming adequate factor dispersion for robust model estimation (Montgomery, 2017). Tensile strength was measured using a universal testing machine (100–300 kN capacity).

#### RSM Methods

The Central Composite Design (CCD) experimental matrix was employed to systematically investigate the effects of welding current (A), voltage (B), and weld speed (C) on the tensile strength of the mild steel. The design comprised twenty experimental runs structured according to a face-centered CCD configuration, incorporating eight factorial points ( $\pm 1$  levels), six axial points ( $\pm\alpha$ , where  $\alpha = 1.0$  for rotatability), and six replicated center points to estimate pure experimental error and assess lack-of-fit. Factor combinations were randomized to mitigate the influence of uncontrolled external variables such as ambient temperature fluctuations or equipment drift, while replication at the design center (Runs 4, 5, 8, 16, 17, 20) enhanced the precision of curvature estimation and provided a robust basis for statistical inference (Box & Wilson, 1951). The orthogonal arrangement of factor levels ensured minimal multicollinearity among regression terms (VIF  $\approx 1.0$ ), thereby facilitating unbiased estimation of linear, interaction, and quadratic effects on responses including HAZ width, dimensional deviation, heat input, and mechanical properties. This experimental framework, implemented via Design-Expert® v13 software, enabled efficient exploration of the three-dimensional design space with minimal resource expenditure while maintaining sufficient degrees of freedom for rigorous ANOVA-based model validation and response surface optimization (Myers et al., 2016).

Equation (1) represents the second-order polynomial regression model fundamental to Response Surface Methodology, where  $Y_{RSM}$  denotes the predicted response,  $\beta_0$  is the intercept term representing the grand mean response at the design center,  $\beta_i$ ,  $\beta_{ii}$ , and  $\beta_{ij}$  are the estimated coefficients for linear, quadratic, and two-factor interaction effects respectively,  $X_i$  are the coded independent variables (current, voltage, weld speed), and  $\varepsilon$  represents the random error term assumed to be normally distributed with zero mean and constant variance (Box & Draper, 1987). The model was fitted using ordinary least squares regression, with coefficient significance evaluated via t-tests at  $\alpha = 0.05$  and overall model adequacy assessed through ANOVA F-tests, lack-of-fit analysis, and diagnostic metrics including Adjusted  $R^2$ , Predicted  $R^2$ , and Adequate Precision ratio (Anderson & Whitcomb, 2016). This parametric formulation provides an interpretable mathematical surrogate for the complex welding process, enabling contour visualization, sensitivity analysis via perturbation plots, and numerical optimization through desirability functions, though its global polynomial structure may exhibit limited flexibility in capturing highly localized nonlinearities inherent to transient thermal-metallurgical phenomena (Khuri & Mukhopadhyay, 2010).

$$Y_{RSM} = \beta_0 + \sum_{i=1}^4 \beta_i X_i + \sum_{i=1}^4 \beta_{ii} X_i^2 + \sum_{i < j}^4 \beta_{ij} X_i X_j + \varepsilon \quad (2)$$

### 3 Results and Discussions

Table 1 presents the complete experimental dataset obtained from the twenty-run Central Composite Design matrix, documenting the measured responses for each unique combination of welding current (180–210 A), voltage (22–25 V), and weld speed (2.0–3.5 mm/s). The tabulated results reveal pronounced sensitivity of tensile strength to variations in the input parameters, with notable trends emerging across the design space: for instance, Run 13 (210 A, 25 V, 2.0 mm/s) yielded tensile strength  $\approx 470$  MPa, confirming experimental repeatability and providing a robust baseline for estimating pure error in subsequent ANOVA procedures. These empirical observations formed the foundational dataset for developing predictive models and establishing causal relationships between process parameters and weldment performance metrics.

Table 1  
Experimental Results

Std	Run	A: Current	B: Voltage	C: Weld speed	Tensile Strength
		I	V	mm/s	MPa
5	1	190	23	2.5	462
8	2	210	22	3.5	432
1	3	180	25	3.5	503
11	4	190	23	2.5	470
17	5	190	23	2.5	474
15	6	190	25	2.5	518
20	7	210	25	3.5	540
7	8	190	23	2.5	477
6	9	180	25	2	448
9	10	200	23	3	509
18	11	210	22	2	428
16	12	180	24	3	430
14	13	210	25	2	516
2	14	200	22	3	450
10	15	210	24	3	477

Std	Run	A: Current	B: Voltage	C: Weld speed	Tensile Strength
19	16	200	24	2	497
4	17	200	24	3.5	532
12	18	180	22	2	425
13	19	180	22	3.5	426
3	20	200	24	3	490

### Modelling and Prediction Analysis

#### RSM Results and Analysis

The quadratic model developed using RSM demonstrated satisfactory predictive capability for Tensile Strength. Table 2 presents the sequential model sum of squares analysis used to identify the most appropriate polynomial order for modeling tensile strength of welded mild steel specimens. The quadratic model was statistically recommended ("Suggested") based on multiple diagnostic criteria: the significant sequential p-value (0.0014) confirmed that inclusion of quadratic terms substantially improved model fit relative to the two-factor interaction (2FI) formulation, while the lack-of-fit p-value (0.0916), though marginally above the conventional  $\alpha = 0.05$  threshold, indicated acceptable agreement between model predictions and pure experimental error. The quadratic model achieved robust goodness-of-fit metrics with an Adjusted  $R^2$  of 0.8698 and a Predicted  $R^2$  of 0.7737, with their difference (0.0961) falling well below the 0.20 threshold recommended for ensuring model generalizability. Although the cubic model exhibited a higher Adjusted  $R^2$  (0.9694), it was designated "Aliased" due to insufficient residual degrees of freedom to independently estimate all higher-order terms, thereby violating the principle of model parsimony and risking overfitting.

Table 2  
Fit Summary for Tensile Strength

Source	Sequential p-value	Lack of Fit p-value	Adjusted $R^2$	Predicted $R^2$	
Linear	0.0009	0.0190	0.5621	0.4164	
2FI	0.4486	0.0175	0.5573	0.1094	
<b>Quadratic</b>	<b>0.0014</b>	<b>0.0916</b>	<b>0.8698</b>	<b>0.7737</b>	<b>Suggested</b>
Cubic	0.0916		0.9694		<b>Aliased</b>

Table 3 presents the Analysis of Variance (ANOVA) for the quadratic Response Surface Methodology model predicting tensile strength, confirming the statistical significance and explanatory power of the developed regression equation. The overall model F-value of 15.11 ( $p = 0.0001$ ) indicates that the model explains a statistically significant proportion of the response variability relative to random noise, with only a 0.01% probability that such an F-ratio could arise by chance alone.

Table 3  
ANOVA for Quadratic model for Tensile Strength

Source	Sum of Squares	df	Mean Square	F-value	p-value	
<b>Model</b>	24398.56	9	2710.95	15.11	0.0001	significant
A-Current	2342.52	1	2342.52	13.05	0.0047	
B-Voltage	13868.38	1	13868.38	77.28	< 0.0001	
C-Weld speed	1240.73	1	1240.73	6.91	0.0252	
AB	1224.53	1	1224.53	6.82	0.0259	

Eyaefe, S., Achebo, J. I., Obahiagbon, K. O., & Etin-Osa, C. E. (2026). Investigation of the effects of some input parameter on the tensile strength of mild steel using RSM. *International Journal of Physical Sciences and Engineering*, 10(2), 7–16. <https://doi.org/10.53730/ijpse.v10n2.15977>

Source	Sum of Squares	df	Mean Square	F-value	p-value	
AC	54.07	1	54.07	0.3013	0.5951	
BC	719.64	1	719.64	4.01	0.0731	
A <sup>2</sup>	5537.17	1	5537.17	30.85	0.0002	
B <sup>2</sup>	198.55	1	198.55	1.11	0.3176	
C <sup>2</sup>	495.66	1	495.66	2.76	0.1275	
<b>Residual</b>	1794.64	10	179.46			
Lack of Fit	1667.89	7	238.27	5.64	0.0916	not significant
Pure Error	126.75	3	42.25			
<b>Cor Total</b>	26193.20	19				

Table 4 summarizes key goodness-of-fit and predictive performance metrics that collectively validate the robustness and practical utility of the quadratic RSM model for tensile strength. The coefficient of determination ( $R^2 = 0.9315$ ) indicates that 93.15% of the total variability in experimental tensile strength measurements was captured by the model, while the Adjusted  $R^2$  (0.8698) accounts for model complexity and confirms that the inclusion of nine regression terms was statistically justified without overfitting. The Predicted  $R^2$  of 0.7737, derived via leave-one-out cross-validation using the PRESS statistic, demonstrates acceptable external predictive capability for this inherently variable mechanical property, with the difference between Adjusted and Predicted  $R^2$  (0.0961) falling below the 0.20 threshold recommended for ensuring model generalizability.

Table 4  
Fit Statistics for Tensile Strength

<b>Std. Dev.</b>	13.40	<b>R<sup>2</sup></b>	0.9315
<b>Mean</b>	475.20	<b>Adjusted R<sup>2</sup></b>	0.8698
<b>C.V. %</b>	2.82	<b>Predicted R<sup>2</sup></b>	0.7737
		<b>Adeq Precision</b>	12.9052

Equation (2) constitutes the empirically derived second-order polynomial model for predicting tensile strength of welded mild steel specimens as a function of the three independent GMAW process parameters expressed in their natural measurement units. The positive linear coefficient for current (+77.98530) indicates that, within the investigated experimental domain, increasing current tends to enhance tensile strength, consistent with improved weld metal consolidation and reduced porosity at optimized energy levels (Lippold & Kotecki, 2005).  $Tensile\ Strength = -3469.99190 + 77.98530A - 310.16366B - 286.63456C + 0.540233AB - 0.225928AC + 8.28291BC - 0.228403A^2 + 4.37911B^2 + 27.33440C^2$  (2) where A represents welding current (A), B denotes voltage (V), and C signifies weld speed (mm/s).

Figure 3 presents the Predicted versus Actual plot for tensile strength, serving as a primary visual validation of the quadratic Response Surface Methodology model's predictive accuracy against experimental measurements. The data points are tightly clustered along the 45° diagonal reference line with minimal systematic deviation, visually corroborating the high coefficient of determination ( $R^2=0.9315$ ) and confirming strong agreement between the model's predictions and the observed mechanical strength values across the entire experimental domain.

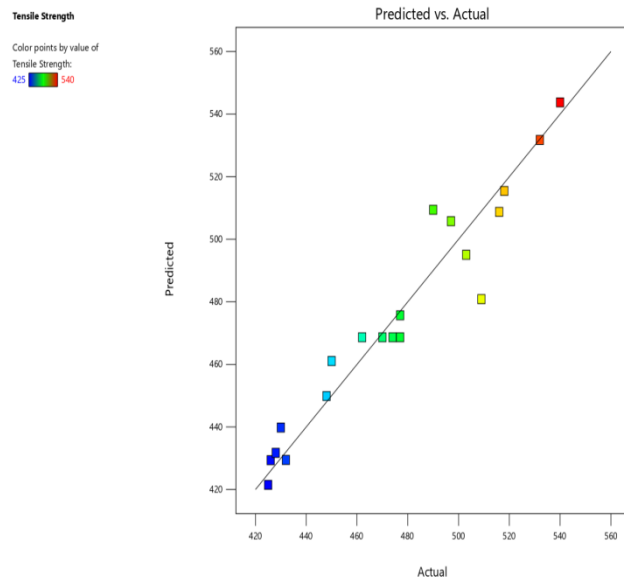


Figure 3: Predicted Vs Actual Plot for Tensile Strength

Figure 4. presents the contour plot for tensile strength as a function of welding current (A) and voltage (B) at a constant weld speed of 2.75 mm/s, providing a two-dimensional topographic representation of the response surface. The plot features a distinct color gradient transitioning from deep blue (minimum strength ~425 MPa) in the lower-left region to bright red/orange (maximum strength >540 MPa) in the upper-central region, clearly delineating zones of optimal mechanical performance. The curvature of the contour lines reflects the significant interaction and quadratic effects identified in the ANOVA, indicating that tensile strength is maximized at intermediate current levels (approx. 195–205 A) combined with high voltage settings.

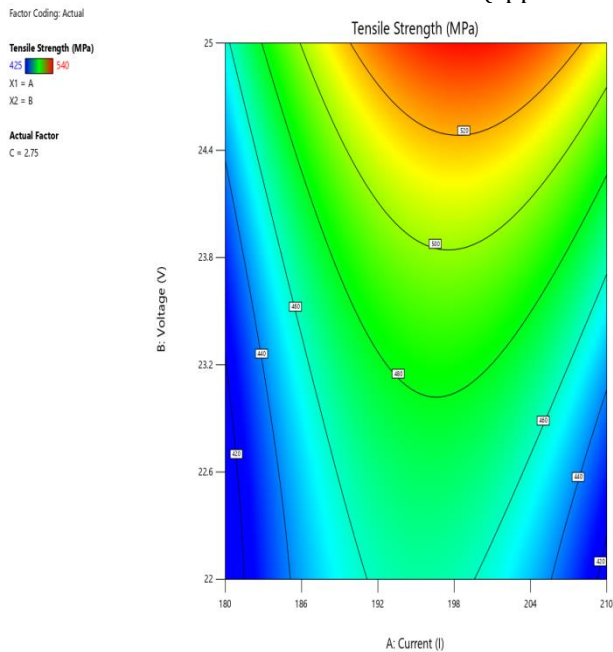


Figure 4: Contour Plot for Tensile Strength

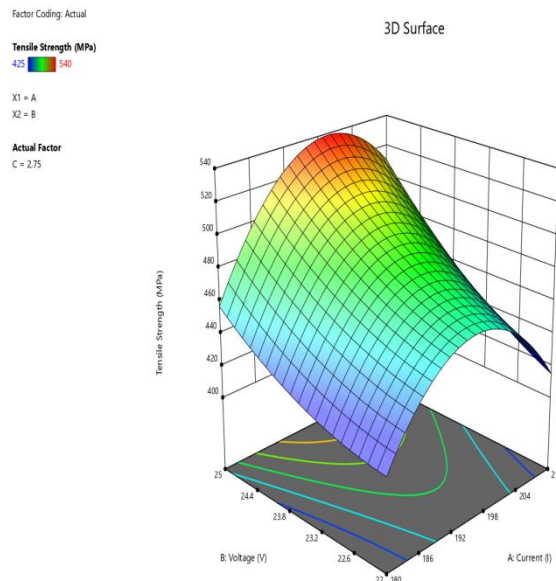


Figure 5: 3D Surface Plot for Tensile Strength

The three-dimensional surface plot (Figure 5) provides a comprehensive geometric visualization of the quadratic RSM model for tensile strength across the current–voltage design plane at a fixed travel speed of 2.75 mm/s. The undulating topology distinctly captures the combined linear and quadratic effects of the process variables, with the surface rising from the lower-left quadrant (low energy input) to a localized peak in the intermediate-current, high-voltage region. The color gradient mapping response magnitude aligns precisely with the contour plot, enabling intuitive interpretation of response gradients and ridge formations that characterize the welding strength landscape.

### Optimization

Table 4 enumerates the top ten optimal solutions generated by the RSM desirability function, all sharing an identical composite desirability of 0.860, which indicates the presence of a broad, flat optimum region rather than a single isolated peak. The minor variations in parameter values (e.g., current ranging from 194.721 to 194.991 A, weld speed from 2.658 to 2.703 mm/s) and corresponding response predictions demonstrate the flexibility and robustness of the optimal operating window. This multiplicity of equivalent solutions provides practical advantages for industrial implementation, allowing welding engineers to select parameters based on secondary constraints such as equipment limitations, productivity requirements, or material batch variations without sacrificing overall weldment quality. Solution 1 was selected as the representative optimum for validation and further analysis, as it offers a balanced compromise with centrally located parameter values that minimize sensitivity to minor process fluctuations while consistently achieving the target geometric and mechanical performance criteria (Supardi et al., 2018).

Table 4  
Optimization Solutions for RSM

Number	Current	Voltage	Weld speed	Toughness	
<b>1</b>	<b>194.853</b>	<b>25.000</b>	<b>2.684</b>	<b>138.375</b>	<b>Selected</b>
2	194.841	25.000	2.678	138.361	
3	194.784	25.000	2.690	138.350	
4	194.865	25.000	2.673	138.365	
5	194.925	25.000	2.694	138.423	
6	194.732	25.000	2.679	138.310	
7	194.991	25.000	2.683	138.439	
8	194.991	25.000	2.671	138.423	
9	194.721	25.000	2.703	138.337	
10	194.764	25.000	2.658	138.295	

## 4 Conclusion

This study successfully investigated the optimization and prediction of the effect of voltage, current, and welding speed on the tensile strength of mild steel using Response Surface Methodology. The results conclusively demonstrated that welding parameters, particularly current, voltage, and travel speed, exert statistically significant and nonlinear influences on weld quality, with voltage emerging as the dominant factor governing heat input, tensile strength, and impact toughness. Experimental validation under optimized conditions confirmed that the identified parameter window (Current  $\approx$ 194–195 A, Voltage = 25 V, Weld Speed  $\approx$ 2.7–3.5 mm/s).


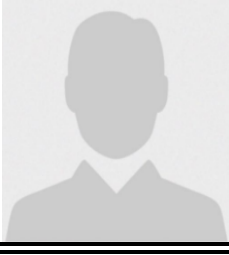
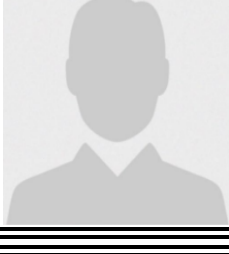
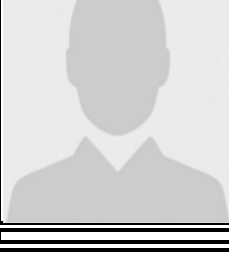
### Acknowledgments

We are grateful to two anonymous reviewers for their valuable comments on the earlier version of this paper.

## References

- Achebo, J. I. (2011). Augmentation of carburized mild steel weld properties to control chafing incidence. *UNIZIK Journal of Engineering and Applied Sciences*, 7(1), 88-92.
- Achebo, J. I. (2012). Effects of Heat Input on the Chemical Composition and Hardness of Mild Steel Weld. *Nigerian Journal of Technology*, 31(2), 213-218.
- Achebo, J. I., & Omoregie, M. J. (2013). Optimum Evaluation of Thermal Performance Characteristics of Micro Heat Pipe using the Hadamard Matrix Design Technique. *International Journal of Engineering Science and Technology*, 5(6), 1254.
- Achebo, J., & Odinikuku, W. E. (2015). Optimization of gas metal arc welding process parameters using standard deviation (SDV) and multi-objective optimization on the basis of ratio analysis (MOORA). *Journal of Minerals and Materials Characterization and Engineering*, 3(4), 298-308.
- Anderson, M. J., & Whitcomb, P. J. (2016). *RSM simplified: optimizing processes using response surface methods for design of experiments*. Productivity press.
- Box, G. E. P. & Wilson, K. B. (1951) On the Experimental Attainment of Optimum Conditions. *Journal of the Royal Statistical Society Series B: Statistical Methodology*, 13, 1-38.
- Box, G. E., & Draper, N. R. (1987). *Empirical model-building and response surfaces*. John Wiley & Sons.
- Khuri, A. I., & Mukhopadhyay, S. (2010). Response surface methodology. *Wiley interdisciplinary reviews: Computational statistics*, 2(2), 128-149.
- Lippold, J. C., & Kotecki, D. J. (2005). *Welding metallurgy and weldability of stainless steels* (p. 376).
- Liu, H. J., Hou, J. C., & Guo, H. (2013). Effect of welding speed on microstructure and mechanical properties of self-reacting friction stir welded 6061-T6 aluminum alloy. *Materials & Design*, 50, 872-878. <https://doi.org/10.1016/j.matdes.2013.03.105>
- Montgomery, D. C. (2017). *Design and analysis of experiments*. John Wiley & sons.
- Myers, R. H., Montgomery, D. C., & Anderson-Cook, C. M. (2016). *Response surface methodology: process and product optimization using designed experiments*. John Wiley & Sons.
- Palani, P. K., & Murugan, N. (2006). Selection of parameters of pulsed current gas metal arc welding. *Journal of Materials Processing Technology*, 172(1), 1-10. <https://doi.org/10.1016/j.jmatprotec.2005.07.013>
- Rao, R., & Yadava, V. (2009). Multi-objective optimization of Nd: YAG laser cutting of thin superalloy sheet using grey relational analysis with entropy measurement. *Optics & Laser Technology*, 41(8), 922-930. <https://doi.org/10.1016/j.optlastec.2009.03.008>
- Sada, S. O. O., Achebo, J., & Obahiagbon, K. (2021). Evaluation of the optimal strength and ductility of a mild steel arc welded plate based on the weld design. *Welding International*, 35(7-9), 261-268.
- Supardi, I. W., Suarabawa, K. N., Wibawa, I. M. S., Padmika, M., Mahayani, N. W. D., & Saputra, I. W. W. (2018). Utilizing turbine ventilator as supplier of electrical energy resources for home information. *International Journal of Physical Sciences and Engineering*, 2(2), 1-10. <https://doi.org/10.29332/ijpse.v2n2.127>

## Biography of Authors

	<p><b>Eyaefe Sunday</b> Department of Production Engineering, University of Benin, Benin City, Nigeria <i>Email: <a href="mailto:eyasunnygee@gmail.com">eyasunnygee@gmail.com</a></i></p>
	<p><b>Achebo J. I</b> Department of Production Engineering, University of Benin, Benin City, Nigeria</p>
	<p><b>Obahiagbon K. O</b> Department of Chemical Engineering, University of Benin, Benin City, Nigeria</p>
	<p><b>Etin-Osa C. E</b> Department of Production Engineering, University of Benin, Benin City, Nigeria</p>